Physiol Genomics 23: 275–286, 2005.
First published September 13, 2005; doi:10.1152/physiolgenomics.00075.2005.

A temporal study of gene expression in rat lung following fixed-volume hemorrhage

P. D. Bowman, J. L. Sondeen, B. Zhao, V. G. Coppes, J. J. Nelson, M. A. Dubick, and G. M. Vaughan
United States Army Institute of Surgical Research, Fort Sam Houston, Texas

Submitted 31 March 2005; accepted in final form 28 August 2005

Bowman, P. D., J. L. Sondeen, B. Zhao, V. G. Coppes, J. J. Nelson, M. A. Dubick, and G. M. Vaughan. A temporal study of gene expression in rat lung following fixed-volume hemorrhage. *Physiol Genomics* 23: 275–286, 2005. First published September 13, 2005; doi:10.1152/physiolgenomics.00075.2005.—Previous studies have indicated that hemorrhage may predispose the lung to respiratory distress syndrome. Gene expression profiling with oligonucleotide microarrays was used to evaluate the genetic responses of the lung to hemorrhage. Conscious rats, chronically instrumented with a catheter and telemetry device to record blood pressure, heart rate, and temperature, had 40% of their estimated blood volume removed at a rate of 1 ml/min over 7–10 min. Groups of three or more rats were euthanized at 1, 3, 6, 16, 24, 48, or 72 h following hemorrhage. Two additional groups were unmanipulated controls and instrumented animals with sham hemorrhage. Total RNA was isolated from lung, reverse-transcribed to cDNA, fluorescently labeled, and hybridized to oligonucleotide microarrays probing 5,671 rat genes. After hemorrhage, statistically detectable alteration of expression was seen in ~0.8% of the genes at some time during the 72-h test period (vs. sham hemorrhage) as determined by false discovery rate statistics in the statistical analysis of microarrays program. A subset was confirmed by RT-PCR analysis. Hemorrhage influenced genes that regulate intracellular signaling and structure, growth factors, and hormonal receptors. There also appeared to be increased expression of genes that may mediate sequestration of neutrophils and mononuclear cells from the circulation. This hemorrhage model, although producing severe hemodynamic alterations, avoided mortality and histological evidence of lung damage, a feature intended to help ensure reliable evaluation of gene expression. These results indicate that gene expression profiling with microarrays provides a new tool for exploring the response of a tissue to systemic blood loss.

gene expression profiling; ischemic lung injury

TRAUMA RESULTING FROM accidental injuries is the leading cause of death in individuals aged 1–44 yr (36), and hemorrhage leading to hypovolemic shock affects 36–39% of trauma victims (23, 25). In addition, ~80% of military casualties experience significant blood loss (20). Despite what appears to be adequate fluid volume resuscitation in these patients, many develop multiple organ failure (MOF), the leading cause of death in the intensive care unit (12). Respiratory failure is most frequent in those who go on to die of MOF.

The importance of the lung as a target following trauma is underscored by the fact that it is the predominant organ to fail in humans after severe trauma in other locations of the body (8). In animal models, hemorrhage (2, 3, 26, 28, 41) produces lung injury or augments lung injury induced by trauma elsewhere. A considerable body of evidence suggests that neutrophil accumulation in the lung is the prime effector of this injury and that the lung actively participates in recruitment of such cells (1, 9–11, 18, 19, 24, 27, 30, 35). In addition, the capillary endothelium of the lung becomes leaky, and the normal alveolar-capillary barrier is disrupted. Some evidence suggests that factors produced by the gut and secreted into lymph arrive at the lung (7, 14, 15, 22, 42) to effect these changes or are derived as products in blood after passage through the liver (31, 37), resulting in complement activation and infiltration of neutrophils and other immune cells. Other recent research has focused on free radicals, proteinases, and soluble agents including cytokines, arachidonic acid metabolites, and charged proteins as possible mediators of lung injury; all may be involved to some degree. The gene responses that the lung makes during this altered condition, however, are largely unknown. It would be useful to understand the responses that the lung makes to hemorrhage to develop strategies for minimizing long-term damage.

The inflammatory response involves a widely accepted model of transcriptional regulation in which genes for cytokines and other inflammatory regulators are transcribed and translated to alter homeostatic mechanisms following injury. Much remains to be done, however, to determine the specific responses that tissues make to injury. Recent advances in genomics are dramatically augmenting investigation of changes in transcriptional activity by a cell or tissue.

With the exception of the report by Alam et al. (4), changes in the global genomic profiling as a function of time after hemorrhage have not heretofore been reported. The purpose of this study is to assess genetic responses of the lung to hemorrhage by use of gene expression profiling with high-density oligonucleotide microarrays. More specifically, the intentions were *1*) to detect a small number of genes among which the proportion with altered expression after hemorrhage is statistically high; *2*) to expand detection of alteration with less-stringent cluster analysis to identify genes appearing to be related by patterns of change; and *3*) to perform these analyses in a model of severe hemorrhage that, nevertheless, is survivable without gross lung damage. We used such a model to optimize RNA preservation for analysis of gene expression related to the lung or to the influx of inflammatory cells. The lung was chosen because it responds to systemic hemorrhage or trauma with influx of inflammatory cells, and in its response resides the potential for development of respiratory distress syndrome.

The long-term goal of this research is a comprehensive understanding of the inflammatory response and means to regulate it for the benefit of the patient with traumatic injuries. The underlying potential of gene expression profiling for studying the progression of inflammation is identification of

Article published online before print. See web site for date of publication (http://physiolgenomics.physiology.org).

Address for reprint requests and other correspondence: P. D. Bowman, US Army Institute of Surgical Research, 3400 Rawley E. Chambers Ave., Bldg. 3611, Fort Sam Houston, TX 78234-6315 (e-mail: phillip.bowman@amedd.army.mil).

Report Documentation Page

Form Approved
OMB No. 0704-0188

1. REPORT DATE	2. REPORT TYPE	3. DATES COVERED
01 DEC 2005	**N/A**	**-**

4. TITLE AND SUBTITLE	5a. CONTRACT NUMBER
A temporal study of gene expression in rat lung following fixed-volume hemorrhage	5b. GRANT NUMBER
	5c. PROGRAM ELEMENT NUMBER
6. AUTHOR(S)	5d. PROJECT NUMBER
Bowman P. D., Sondeen J. L., Zhao B., Coppes V. G., Nelson J. J., Dubick M. A., Vaughan G. M.,	5e. TASK NUMBER
	5f. WORK UNIT NUMBER
7. PERFORMING ORGANIZATION NAME(S) AND ADDRESS(ES)	8. PERFORMING ORGANIZATION REPORT NUMBER
United States Army Institute of Surgical Research, JBSA Fort Sam Houston, TX 78234	
9. SPONSORING/MONITORING AGENCY NAME(S) AND ADDRESS(ES)	10. SPONSOR/MONITOR'S ACRONYM(S)
	11. SPONSOR/MONITOR'S REPORT NUMBER(S)

12. DISTRIBUTION/AVAILABILITY STATEMENT
Approved for public release, distribution unlimited

13. SUPPLEMENTARY NOTES

14. ABSTRACT

15. SUBJECT TERMS

16. SECURITY CLASSIFICATION OF:			17. LIMITATION OF ABSTRACT	18. NUMBER OF PAGES	19a. NAME OF RESPONSIBLE PERSON
a. REPORT	b. ABSTRACT	c. THIS PAGE			
unclassified	**unclassified**	**unclassified**	**SAR**	**12**	

Standard Form 298 (Rev. 8-98)
Prescribed by ANSI Std Z39-18

those genes whose expression may be altered pharmacologically and thus targeted for control.

MATERIALS AND METHODS

Surgical preparation of animals. Animal experiments were performed in accordance with the National Institutes of Health (Bethesda, MD) Guide for the Care and Use of Laboratory Animals with approval of the United States Army Institute of Surgical Research Animal Care and Use Committee. Male Sprague-Dawley rats weighing 280–300 g were observed for at least 1 wk in a 12:12-h light-dark cycle (lights on 6 AM) following arrival at the vivarium to allow for adjustments to environmental changes and to exclude the possibility of preexisting disease. Anesthesia was induced in a Plexiglas chamber with 5% isoflurane, and the rat was then maintained at 1.75–2.5% isoflurane through a nose cone via a Bain circuit and rodent gas anesthesia machine (VetEquip, Pleasanton, CA). Sham and hemorrhaged rats were instrumented with two arterial catheters, one externalized for blood withdrawal and the other connected to an indwelling Data Sciences International (DSI) PhysioTel (St. Paul, MN; model C50-PXT) monitoring device placed intraperitoneally and used in monitoring blood pressure, temperature, and electrocardiogram data via telemetry. For their placement, a midline abdominal incision was made through the skin and peritoneum and the aorta exposed by blunt dissection.

The externalized catheter (0.040-in. outer diameter micro-RenaPulse catheter; Braintree Scientific, Braintree, MA), coated with 2% tridodecylmethylammonium heparinate solution (Polyscience, Warrington, PA), was routed through a stab wound in the skin at the nape of the neck. A silk suture was passed around the aorta infrarenally immediately before insertion of the catheter to control bleeding. The distal end of the left iliac artery was ligated and the catheter was advanced through a puncture made with a 21-gauge bent needle, so that the catheter tip lay in the aorta just caudal to the renal arteries. A second ligature secured the catheter in the iliac artery. The pressure-monitoring DSI catheter was inserted nonocclusively through the right iliac artery and its tip advanced to ~1 cm caudal to the tip of the first catheter in the infrarenal aorta. The catheter was then secured with a drop of tissue adhesive and a cellulose patch. The abdominal incision was closed in layers, and the battery pack was anchored to the abdominal wall with one 4-0 suture. The skin was closed with skin staples.

The externalized catheter was attached to a pump (Harvard Apparatus, model 22) via a rodent swivel (23 ga) and tether (12 in.) apparatus (Lomir Biomedical, Notre-Dame-de-l'Ile-Perrot, Quebec, Canada). Heparinized saline (5 U/ml) with penicillin G (1,054 U/ml) was infused continuously at 0.5 ml/h to maintain patency and prevent contamination of the catheter. After 7–10 days of recovery, and only after the animals had begun to gain weight, the experiment was performed. On the day prior to hemorrhage, the continuous infusions were switched to saline (0.9%) to remove residual heparin and antibiotics before the hemorrhage period. Immediately before hemorrhage, the maintenance saline infusion was discontinued.

Experimental procedures. Telemetered physiological data were recorded for a 10-min baseline period before hemorrhage in all animals, and in all uneuthanized animals before euthanization of a given group in relation to the specified time after hemorrhage. At the start of hemorrhage (H), blood was withdrawn through the catheter with 1-ml syringes at a rate of l ml/min. Total blood volume was estimated to be 6.5% body wt, and 40% of this (2.6 ml/100 g) was removed to produce the hemorrhage, and this blood provided a baseline for hematologic and biochemical measurements. No resuscitation was performed, and all animals survived this level of hemorrhage for the length of the study (1–72 h). Animals were allowed access to food and water. Group coding was: *group 1*, control (Con; no instrumentation or hemorrhage); *group 2*, sham hemorrhage (Sh; instrumentation but no hemorrhage); and *groups 3–9* for various time points after hemorrhage (H1h to H72h). Thus at the end of 1, 3, 6, 16, 24, 48, and 72 h after hemorrhage, separate groups of animals were anesthetized with Nembutal (50 mg/kg) and euthanized by exsanguination when the posthemorrhage blood sample was taken by cardiac puncture. Group sizes were six rats (Sh), five rats (H6h), and three rats (the remaining groups). Hemorrhage was timed so that the groups were euthanized at about the same time of day as was Sh (~4 PM), except for H16h, euthanized at 8 AM. At autopsy, 100 mg of the lung were removed and placed in RNALater (Ambion, Austin, TX). Tissues were collected within 10 min of death.

Hematologic and serum analyses. Blood samples were collected into EDTA tubes (for complete blood cell counts and cell type analysis) or tubes without anticoagulants (for total serum protein and enzyme analysis). Hematocrit (Hct), blood cell counts, and cell types were determined with a Pentra 120 Hematology Analyzer (ABX, Montpellier, France) and analyzed with the supplied veterinary software package according to manufacturer's instructions. All counts and cell type determinations were validated by manual hemocytometer counts and differential staining (methylene blue-eosin stain) followed by quantification.

Analysis of total protein (Total Prot), albumin, aspartate aminotransferase (AST), alanine aminotransferase (ALT), alkaline phosphatase (ALKPhos), and lactate dehydrogenase (LDH) were performed on a Vitros 250 Hematology Analyzer (Ortho-Clinical Diagnostics, Rochester, NY) per the manufacturer's instructions.

Lung myeloperoxidase assay. Lung myeloperoxidase (MPO) activity was determined by a modification of the method of Trush et al. (33). Lung samples were homogenized in 50 mM potassium phosphate buffer, pH 6.0, containing 0.5% hexadecyltrimethylammonium bromide. The samples then underwent three freeze-thaw cycles and sonification, followed by incubation in a 60°C water bath for 2 h to extract MPO and eliminate interfering substances. Samples were then centrifuged at 10,000 *g* for 30 min at 4°C. MPO activity was determined in the resultant supernatant, using *o*-dianisidine as substrate. Protein concentration of the lung homogenates was determined using a commercial kit (BioRad Laboratories, Richmond, CA).

Histology. At necropsy, 0.5× 1-cm blocks of liver and lung tissue fixed in neutral buffered formalin were processed into paraffin and sectioned at 5 μm. After hematoxylin and eosin staining, they were examined for morphological alterations by light microscopy.

Microarray procedures. Each oligonucleotide in the rat v1.1 array-ready oligonucleotide set (70 nucleotides in length) from Qiagen (Chatsworth, CA) was reconstituted at 20 mM in 150 mM sodium phosphate buffer (pH 8.5), and microarrays were spotted in duplicate with an Omni Accent arrayer (GeneMachines, San Carlos, CA) using Stealth SMP3 pins (Telechem International, Santa Clara, CA) on aldehyde-treated microscope slides (Cel Associates, Pearland, TX).

Total RNA was isolated from the lung of each animal with two rounds of TRI Reagent (MRC, Cincinnati, OH), and its quality was analyzed by gel electrophoresis. A reference preparation consisting of equal amounts of RNA pooled from nine organs (liver, lung, kidney, spleen, heart, skeletal muscle, skin, jejunum, and brain) of untreated control animals was used as reference RNA. Five-microgram samples exhibiting undegraded RNA from each rat lung were reverse transcribed with Superscript II (Invitrogen, Carlsbad, CA) in the presence of a C-6 amine-modified random hexamer and aminoallodeoxyuridine to produce fluorescent-labeled cDNA as described (40). RNA from the reference preparation was all labeled together. After reverse transcription, RNA was degraded by addition of 1 N NaOH to yield 0.1 M NaOH and heated to 65°C for 15 min and then neutralized with ph 7.0 HEPES buffer. After isolation on Qiaquick columns (Qiagen), elution, and lyophilization, the lung sample was labeled with Cy5 ester and reference cDNA samples with Cy3 ester (Amersham Biotech, Piscataway, NJ). After separation from unbound dye, the samples were again lyophilized and then reconstituted in hybridization solution [32% formamide, 5× Denhardt's solution, 3× saline sodium citrate (SSC), 20 mM HEPES buffer, pH 7.0] and hybridized to

Table 1. *RT-PCR*

Gene	GeneBank Accession No.	Forward Primer	Reverse Primer
Angiopoietin 1 (AP1)	NM_053 546	AACGGGGAGAGCGTCAAACAAC	TGCAGCTCCTCCATAGTGAA
L-Gicerin (GIC)	NM_023983	GGCCCTTCTGAAGTGTGG	TGCCTCTCCTTGTGAATCAA
Guanine nucleotide-binding protein (GNBP)	NM_024138	GCACAGTATTTCTCTTCCAGGGTG	ACCAACCAGCAAGGGGTCATTC
Interleukin 2 (IL2)	M22899	CTGCAAAGGAAACACAGCAG	TGGGGAGTTTCAGATTCTTGTAAT
Neutrophil collagenase (NeuCol)	NM_022221	ACCACTTACCAAGCAATCAGTTCC	AGAAATCACCAGAGTCGGGCAC
Pyruvate dehydrogenase kinase 1 (PDK1)	L22294	TTCCCGATAATCTTCTCAGGACC	GAACATTTTGGCTGGTGACAGG
Ribosomal protein L10a (RP L10a)	NM_031065	CCTGCTGACACACAATGAAAA	AACGGCCAGACACAGCAC
Xanthine dehydrogenase (XDH)	NM_017154	TGCCATTGATATTGGACAAGTAG	TGCAGCTCCTCCATAGTGAA
β-Actin	BC013835	TTCTACAATGAGCTGCGTGTGG	TACATGGCTGGGGTGTTGAAGG

microarrays for 20 h at 42°C. After hybridization on a microarray (1 per rat), a washing to remove unhybridized cDNA, and scanning with an Axon 4000B (Axon Instruments, Union City, CA) at 10-μm resolution, the resulting 16-bit TIFF images were analyzed with GenePix 4.1 software (Axon Instruments) for calculation of Cy5 and Cy3 fluorescence intensities at each spot.

RT-PCR. RT-PCR was performed in a subset of those 425 genes entered into the clustering program because of posthemorrhage expression alteration suggested by passing at least one two-group statistical analysis of microarrays (SAM) comparison of microarray results (see hierarchical clustering under *Data analysis*). After the results of clustering were available, eight genes were selected to represent each of the three upregulated clusters as well as a diversity of gene functions. RT-PCR was performed on the lung samples from the three animals of the H3h group and three Sh rats.

PCR reactions were performed with use of a LightCycler thermal cycler (Idaho Technology, Salt Lake City, UT) in the H3h and Sh groups with 1 μg of total RNA from the same samples used for microarray analysis. Total RNA was reverse transcribed to cDNA with Superscript III RT and random hexamer priming (Life Technologies), and 1 μl of the cDNA solution was amplified with LightCycler FastStart Master Sybr Green I master mix (Roche Diagnostics, Indianapolis, IN) in a 10-μl reaction with a primer set for each gene and synthesized by Midland Certified Reagent (Midland, TX; Table 1).

The course of the amplification reaction was followed with the LightCycler software and stopped during the exponential phase for each gene. All the resultant PCR products were separated by gel electrophoresis on 2–3% agarose containing 1:10,000 Sybr gold nucleic acid stain (Molecular Probes, Portland, OR). The image was captured with GelPro 4.3 software (Media Cybernetics, Silver Springs, MD), and the integrated optical density (intensity), calculated automatically for each lane, was normalized to that for β-actin in each sample.

Data analysis. Hemodynamic, hematologic, and biochemical data were analyzed by one-way or two-way ANOVA (time and treatment as factors). Post hoc two-tailed *t*-tests were used to compare two time points. $P < 0.05$ was considered significant.

For gene profiling by microarray, Cy5 dye (635-nm excitation) was used to label DNA representing the lung tissue separately for a given rat. Cy3 dye (532-nm excitation) was used to label the standard pool of reference cDNA. Labeled DNA from each rat's lung (incubated separately with 1 microarray) and from the standard pool (the same reference DNA in all incubations) was hybridized to a given microarray simultaneously. For a given microarray, data were acquired (GenePix Pro 4.1) as the separate median intensity of Cy5 and Cy3 emission in the pixels at each spot after laser excitation, minus the respective Cy5 or Cy3 median background intensity taken from a standard area around the spot. Cy5 and Cy3 intensities were normalized (within each microarray) to their respective overall mean and then rescaled to produce an overall geometric mean Cy5-to-Cy3 ratio of one for the array. Each gene was represented by a pair of spots, yielding duplicate-mean normalized intensities for Cy5 and for Cy3 as the data. For assessment of variability and detection, each microarray contained 451 pairs of buffer spots (blanks) and 12–16 pairs of spots for each of 12 separate randomly generated negative controls (RGNCs) from the Qiagen Rat Genome Set v1.1, presumably all mismatches to the known rat gene sequences. All evaluated data were normalized pair means (cases) for Cy5 and Cy3. For analyses, a filtration process removed genes (or RGNC cases) whose Cy5 or Cy3 mean across all arrays was below the 95 percentile of that for the blanks (5.6% of the 5,671 genes or expressed sequence tags were thus excluded).

Log (base 2) values of the Cy5-to-Cy3 ratio for all remaining genes on all the arrays were entered into the program SAM (34) (v1.21, **http://www-stat.stanford.edu**) as a Microsoft Excel add-in. First, the empiric permutational one-way ANOVA (multiclass response test) was performed to generate a list of genes likely to be changed across the nine rat groups. Then, empiric permutational *t*-tests between two rat groups (two class, unpaired data test) were performed, again on all the genes. Each such test compared one posthemorrhage time point to Sh at each gene.[1] The number of permutations was set at 1,000 for each SAM test. A gene's *q* value for a comparison is lower with a higher observed error-adjusted between-group difference (higher observed effect size). The *q* threshold for significance is the false discovery rate (FDR; the estimated no. of significant genes with no true difference as a proportion of all those called significant). The FDR is set by the investigator entering a value ("delta") to represent the effect size threshold producing the desired *q* threshold (the desired FDR). In conformity with the purpose of microarray use, i.e., to provide a screening test identifying a short list of significant genes with a small proportion having no real underlying effect (low FDR), this meaning of significance (the FDR) applies to any one SAM test (any 1 comparison among or between rat groups). However, we required both of two criteria for final detection of alteration in a gene's expression: *1*) *q* value at the minimal obtainable FDR in the permutational ANOVA and *2*) *q* value < 0.05 (producing an estimated FDR

[1] A given comparison is performed at each of a large number of genes. In this context, *p* values and *p* thresholds for significance, even if corrected for multiple comparisons, provide no assessment of the false-discovery rate (FDR) among the genes called significant. Once the proportion of genes with no true difference is estimated (32), and a significance threshold for observed error-adjusted effect size is assigned, then the related *p* threshold represents the estimated number of false-positives (false discoveries, genes called significant without a true difference) expressed as a proportion of the total number with no true difference. In contrast (32), the FDR (also being the *q* threshold for significance) is estimated by the same numerator (number of false positives), but expressed, instead, as a proportion of the significant genes. A gene's *q* value (if different from the FDR) is the potential FDR that would be obtained if that gene's own observed error-adjusted effect size would be used as the effect-size threshold (32). Because of the high multiplicity of comparisons (a given comparison being performed at each gene) and the attendant need for FDR assessment, we used not *p* values, but *q* values and the FDR as provided in SAM.

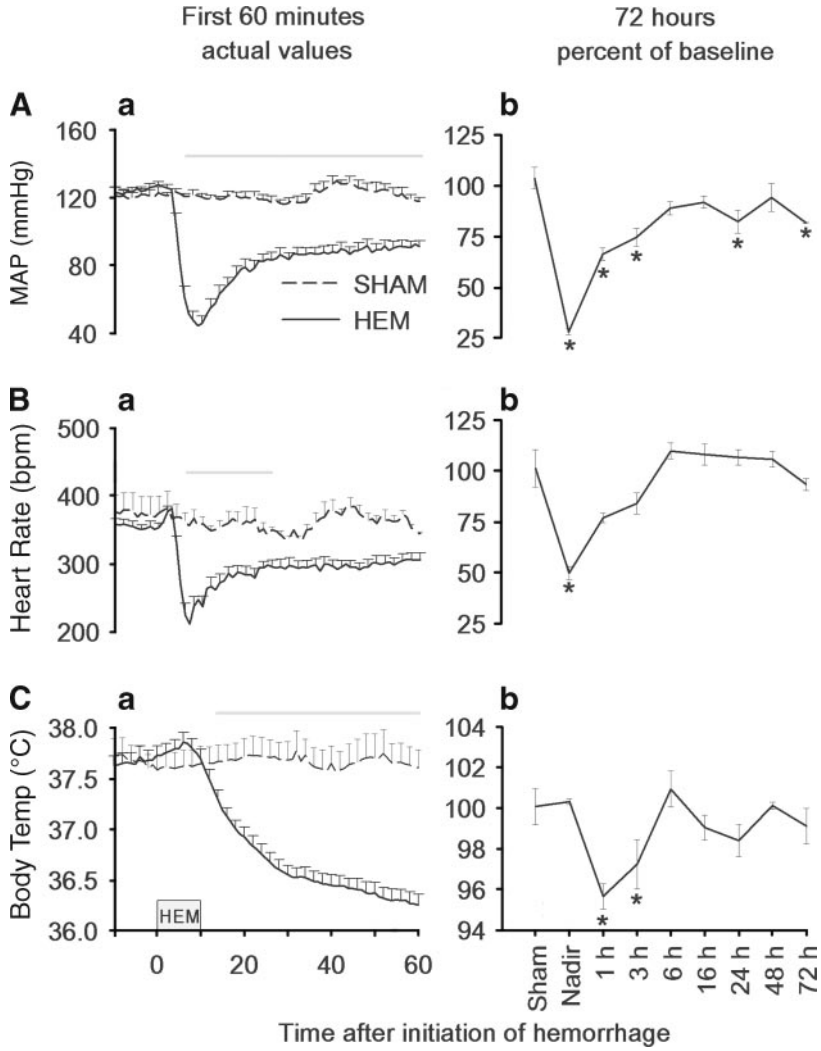

Fig. 1. At *left*, *Aa*, *Ba*, and *Ca* depict the raw values of mean arterial pressure (MAP), heart rate [HR; in beats/min (bpm)], and temperature (Temp), respectively, at 1-min intervals for the first 60 min in the sham (Sham) and hemorrhaged (Hem) groups. The horizontal line above the sham data indicates where each of the hemorrhage means is significantly lower than the sham mean at the same time point. *Ca*, *inset*: box with "Hem" depicts hemorrhage period. At *right*, *Ab*, *Bb*, and *Cb* depict the MAP, HR, and Temp as percentage of baseline for each of the 7 hemorrhaged groups. The nadir point included values from all the animals. Note the different time scale (h). $*P < 0.05$, each hemorrhaged group vs. sham. Data are means ± SE.

of 5%) at one or more time points posthemorrhage vs. Sh in the permutational *t*-tests between two groups. Among the genes in a short list obtained in this fashion, the final FDR is not known, but should be more conservative than that used in either criterion alone. No folding-ratio criterion was used at any step in this process. All the microarray data have been deposited at the Gene Expression Omnibus (**http://www.ncbi.nlm.nih.gov/geo/**; GPL968) in a minimum information about a microarray experiment (MIAME)-compliant format. More details of our microarray data reduction, analyses, and results can be found as Supplemental Material ("Rat Lung Gene Microarrays after Hemorrhage;" available at the *Physiological Genomics* web site).[2]

Hierarchical clustering was performed on the microarray data for all genes passing (significant in) the SAM two-group test at one or more time points vs. Sh [Cluster and Treeview software (8)]. A datum for this procedure was the log (base 2) of the folding ratio at each relevant gene for each time posthemorrhage, where the folding ratio was the geometric mean of Cy5/Cy3 for a rat group at a given time divided by the geometric mean of Cy5/Cy3 for Sh.

With regard to the RT-PCR data, the base 2 logs of the normalized intensities were used for *t*-test comparison between the two groups with respect to a given gene. The geometric mean of the normalized values for a given gene within the H3h group was divided by the comparable geometric mean from the Sh group to express the folding change (i.e., the ratio of geometric means) at 3 h after hemorrhage. Similarity between the RT-PCR and microarray results for these genes was assessed by the Pearson correlation coefficient.

RESULTS

Physiological measures. The removal of 40% of the estimated blood volume of a conscious rat resulted in a rapid drop in mean arterial blood pressure (MAP) from ~120 to ~40 mmHg (Fig. 1*Aa*). The hemodynamic responses were averaged over the first posthemorrhage hour for each animal, and there were no differences among the hemorrhaged groups, demonstrating that this hemorrhage procedure is highly reproducible (Fig. 1*Aa*). Within 10 min, compensatory mechanisms began to elevate blood pressure, and the MAP typically returned to ~80% of baseline within 6–12 h (Fig. 1*Ab*).

Rapid hemorrhage also induced a bradycardic response during the blood withdrawal phase (Fig. 1*Ba*), but the heart rate returned toward baseline levels within 30 min and remained there for the 72-h period (Fig. 1*Bb*). Maximum reduction in core temperature occurred at ~1 h after hemorrhage (Fig. 1*Ca*) and started to return to within 0.5°C of the baseline temperature in most animals by 6 h (Fig. 1*Cb*).

[2] The Supplemental Material for this article is available online at **http://physiolgenomics.physiology.org/cgi/content/full/00075.2005/DC1**.

Table 2. *Baseline values for hematologic and serum protein data*

Variable	Units	Baseline Values
Hct	% as RBC	37.6±0.4
RBC	10^6/ml	7.2±0.1
WBC	10^3/ml	10.0±0.5
Platelets	10^3/ml	664±33
Lymphocytes	10^3/ml	7.2±0.4
Neutrophils	10^3/ml	2.1±0.2
Lymphocytes	%	71±1
Neutrophils	%	22±1
Total protein	g/dl	5.2±0.1

Baseline values for hematologic and serum protein data, expressed as means ± SE. WBC, white blood cells; RBC, red blood cells; Hct, hematocrit.

Hematologic and serum analyses. Baseline Hct, cell counts, and serum protein are shown in Table 2. Figure 2*A* shows that the Hct was reduced by ~40% within the first hour and started to recover only at 72 h. This indicates that recruitment of intracellular and interstitial fluid into the vascular space was complete within 1 h after hemorrhage. Within 6 h, plasma protein concentration started to increase, returning to baseline levels by 48 h (Fig. 2*A*). Figure 2*B* shows a significant increase in the ratio of total protein to Hct. This recovery probably was due to redistribution of interstitial protein into the vascular space as well as synthesis of new protein. The ~60% reduction from baseline at 1 h in the numbers of white blood cells (WBC) (Fig. 2*C*), lymphocytes (Fig. 2*E*), and neutrophils (Fig. 2*E*) exceeds the 40% reduction in red blood cells (RBC) (Fig. 2*C*), which may reflect sequestration of the lymphocytes and neutrophils in the immediate posthemorrhage period (Fig. 2*C*). In contrast, the number of platelets was not reduced, indicating that their numbers were increased relative to that expected due to the loss from the hemorrhage, as shown by the increase in the ratio of platelets to RBC vs. the ratio of WBC to RBC (Fig. 2*D*). By 72 h, the numbers of WBC, neutrophils, and lymphocytes were significantly increased compared with the baseline (Fig. 2, *C–E*). As seen in Figure 2*F*, the proportion of lymphocytes and neutrophils that made up the total WBC did not change in response to hemorrhage.

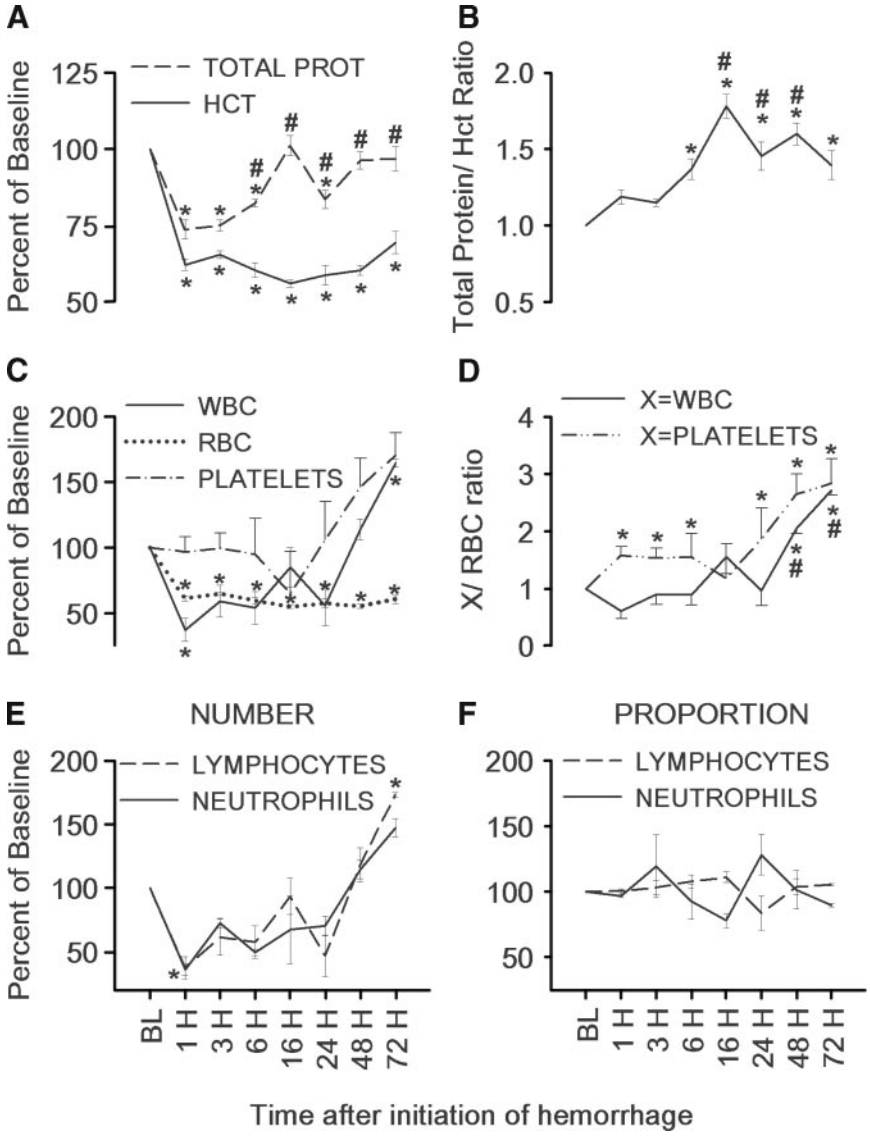

Fig. 2. *A*: hematocrit (Hct) and total serum protein (Total Prot) as percentage of baseline. *B*: ratio of the Total Prot to Hct. *C*: no. of white blood cells (WBC), red blood cells (RBC), and platelets as percentage of baseline. *D*: either the WBC-to-RBC or platelets-to-RBC ratio. *E*: no. of lymphocytes and neutrophils as a percentage of baseline (the ordinate axis label for *E* also applies to this panel). *$P < 0.05$, different from baseline. #$P < 0.05$, different from the 1- and 3-h time points. Data are means ± SE.

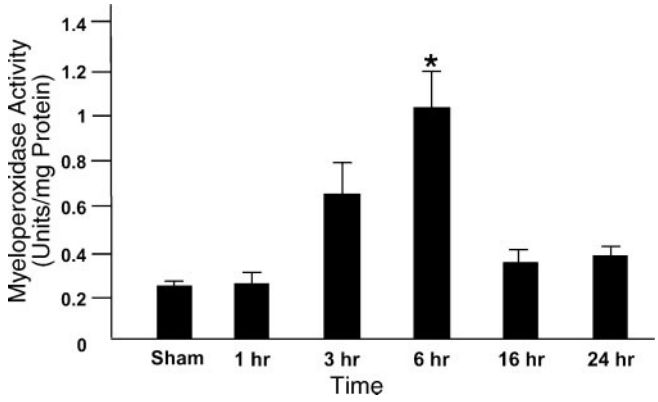

Fig. 3. Myeloperoxidase activity in lung after hemorrhage. Values are means ± SE. *$P < 0.05$ for the 6-h group vs. sham.

There were no significant changes in serum activity of hepatic enzymes (AST, ALT, LDH, ALKPhos) (data not shown).

Lung myeloperoxidase activity. Because immigration of hemopoetic cells into a tissue might lead to gene expression from a foreign cell type, and since neutrophils are thought to be significant participants in the response of lung to hemorrhage, we assessed the degree of neutrophil immigration into the lung. Sufficient material for adequate measurement was available only in the Sh and H1h through H24h groups. At 6 h (Fig. 3), there was increased myeloperoxidase activity indicating the increased presence or activity of neutrophils.

Histology. Necrosis was not seen in light-microscopic preparations of liver. In preparations of lung (with unremarkable alveoli and no evidence of necrosis), we encountered polymorphonuclear cells (compatible with neutrophils), typically in blood vessels (Fig. 4). Although there appeared to be a small posthemorrhage increase in their occurrence (relative to that in Sh), this was not quantified.

Gene expression profiling. Estimated nondetectability of expression (hybridization in the range of nonspecific binding) among genes was addressed with the Cy5 values. The count of genes with a rat group median at or below the respective 95 percentile value for blanks would give an estimate of the fraction of genes having nondetectable expression in that group. The mean value of this fraction across the groups was 7.2%. (This value differs from the 5.6% of genes filtered out before further analysis, because filtration could not depend on a threshold intensity in any one group but depended on a mean value across all arrays at each gene and blank case; see MATERIALS AND METHODS). The RGNCs might also provide an estimate of nonspecific binding. Their low number (12 RGNCs) together with their skewed binding distribution, with some cases showing higher nonspecific hybridization than seen in blanks, meant they were not likely suited for an estimate based on a quantile. However, in that there were many replicates of each RGNC, an accumulative technique was used based on the minimal-frequency fraction of expected P value frequency seen at the highest values of P (see Supplemental Materials), originally developed for estimating the fraction of genes with no true alteration in a comparison (32). In this case, P represented the empiric probability (based on ranks of the pooled RGNC replicates) of a gene's Cy5 magnitude being at that level or higher as a result only of nonspecific (RGNC) binding. This provided an average estimate of nondetectable signal in 9.8% of genes.

For Cy5, Cy3, and the Cy5-to-Cy3 ratio, the within- and between-array standard deviations were positively related to the magnitude such that the respective coefficients of variation (CVs) appeared to be approximately constant over the whole range of magnitude. The estimated within-array CVs were 29% (Cy5), 20% (Cy3), and 20% (Cy5/Cy3). The respective values for between-array (within-group) CVs were 33, 20, and 26%.

The Cy5-to-Cy3 ratio, containing a correction (Cy3) for potentially confounding sources of variation, was taken as the measure of expression for comparative purposes. The most highly expressed genes in the control group were those for surfactant, surfactant-associated protein 1 (pulmonary surfactant protein, SP-A), pulmonary-associated protein B, pulmonary-associated protein C, lysozyme, uteroglobin (Clara cell secretory protein), and A kinase (PRKA) anchor protein 5, reflecting the prominent contribution of mRNA from cells of lung epithelial origin.

Changes in "genes" and "gene expression" are used synonymously throughout. To compare expression across rat groups (time points) within each gene, the data (as Cy5/Cy3) were assessed by the SAM program. The test for any differences across all 9 groups identified 51 significant

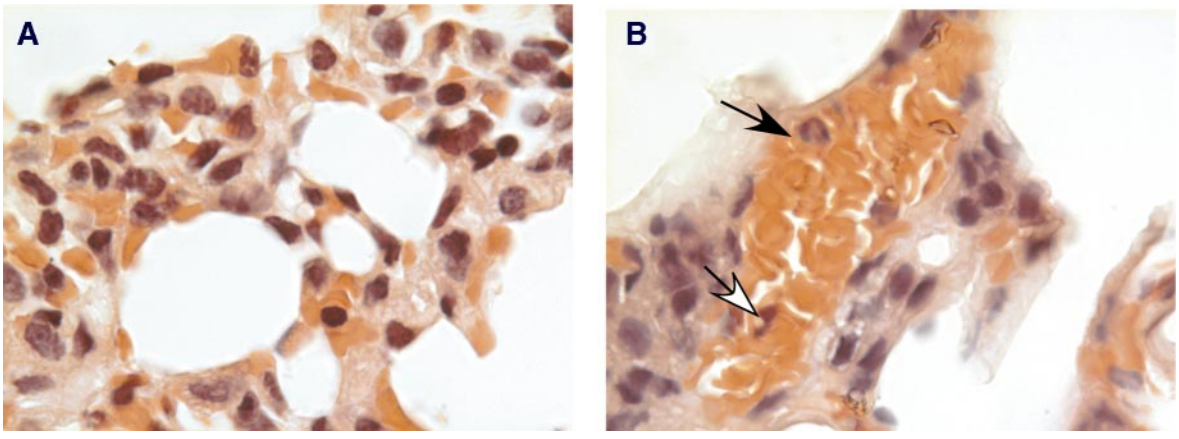

Fig. 4. Photomicrographs of lung from a sham rat (*A*) and a rat at 6 h after hemorrhage (*B*). The small changes in neutrophil no. accompanying the enzyme rise in myeloperoxidase activity were not reliably quantifiable histologically. Arrows indicate neutrophils.

Table 3. *Genes passing the multiclass response test: 2-group comparisons*

List No.	Gene ID	Gene Name	Folding Ratio (Denominator Group) Sh (Con)	H1h (Sh)	H3h (Sh)	H6h (Sh)	H16h (Sh)	H24h (Sh)	H48h (Sh)	H72h (Sh)
1	NM_022221	Neutrophil collagenase	1.31	1.82	**4.81**	**2.11**	1.19	3.62	**5.04**	**18.36**
2	L18948	S100 Ca-binding protein A9 (calgranulin B)	0.76	3.31	**5.26**	2.64	1.30	7.08	**7.35**	**5.53**
3	AI409114	ESTs, similar to nucl receptor coactivator 5	4.27	1.96	3.32	**2.82**	3.09	3.17	**4.84**	**5.11**
4	D50671	GABA receptor rho-3 subunit	1.81	1.20	2.16	**2.18**	2.14	1.76	2.43	**3.06**
5	L40030	Placental growth factor	0.39	4.13	7.74	3.62	1.94	13.04	**16.75**	**11.79**
6	X68657	Mast cell protease 10	1.10	2.07	2.50	2.11	2.11	2.33	**4.08**	**5.79**
7	NM_031065	Ribosomal protein L10a	1.34	1.66	**4.10**	1.78	2.63	2.89	1.82	1.21
8	BG662614	ESTs, similar to T12468 hypothetical protei	5.04	1.55	0.24	**6.46**	5.72	4.73	3.53	3.93
9	BG668837	ESTs, similar to CYCI_MOUSE Cyclin I	14.11	1.97	0.60	**8.28**	9.13	9.67	2.85	6.97
10	V01224	Rat messenger RNA for alpha-actin	1.75	0.92	1.48	**1.77**	1.83	1.95	0.70	0.50
11	NM_012523	CD53 antigen	0.91	1.65	2.07	1.61	0.49	2.23	2.41	**4.38**
12	NM_134462	putative secretory Ca-ATPase SPCA2	0.92	0.88	1.15	1.15	0.98	1.98	2.34	**3.31**
13	NM_023099	G protein-coupled receptor 27	0.82	0.57	**0.31**	**0.49**	0.39	**0.32**	0.47	**0.42**
14	NM_013087	CD81 antigen, target of antiprolif antibody 1	1.18	0.65	0.60	**0.44**	0.20	**0.25**	**0.36**	**0.42**
15	NM_017193	Kynurenine aminotransferase 2	1.36	0.62	0.35	**0.37**	0.65	**0.16**	**0.21**	**0.17**
16	NM_022849	Deleted in malignant brain tumors 1	0.99	0.65	0.37	**0.48**	0.29	**0.17**	**0.27**	**0.37**
17	U49057	CTD-binding SR-like protein rA9	0.92	0.71	0.58	**0.49**	0.35	**0.27**	**0.37**	**0.27**
18	U68172	Mucin 2	1.04	0.78	0.50	**0.57**	0.51	**0.31**	**0.39**	**0.52**
19	AI575729	ESTs, sim to hypothet protein, MNCb-1301	0.79	0.91	0.27	**0.42**	0.34	**0.28**	0.50	**0.36**
20	X77817	R.norvegicus VCS-α2 mRNA for SMR1-α2	0.52	1.53	0.62	**0.35**	0.49	**0.25**	0.41	**0.35**
21	NM_012493	Alpha-fetoprotein	1.15	1.01	1.11	**0.44**	0.47	**0.33**	0.53	**0.33**
22	U27322	Arginine vasopressin receptor 1B	0.98	0.79	0.62	**0.57**	0.40	**0.27**	0.44	**0.34**
23	NM_031057	Methylmalonate semialdehyde dehydrogen	1.43	0.64	0.63	**0.39**	0.13	**0.34**	0.45	**0.36**
24	NM_022687	Transcription factor HES-3	1.06	0.96	0.71	**0.51**	0.42	**0.36**	0.42	**0.45**
25	NM_019623	P450, subfam IVF, polypeptide 14 (leukotri	0.95	0.64	0.48	**0.52**	0.29	**0.20**	0.42	0.48
26	NM_031334	Cadherin 1	0.83	0.98	0.48	0.66	0.27	**0.26**	0.38	**0.34**
27	AF277717	Fibroblast growth factor receptor 3	0.97	0.98	0.87	0.94	0.57	**0.42**	0.52	**0.22**
28	M75168	HLA-B-associated transcript 1A	0.74	1.12	0.64	0.77	0.40	**0.34**	0.41	**0.33**
29	NM_031731	Aldehyde dehydrogenase family 3, subf A2	1.02	1.00	0.57	0.61	0.33	**0.31**	0.56	**0.44**
30	AF467250	K+ channel, subf K, member 15 (TASK-5)	0.83	0.70	0.62	0.84	0.41	**0.31**	0.54	**0.44**
31	AJ243123	Cytokine inducible SH2-containing protein 1	0.85	0.64	**0.27**	0.91	0.53	0.33	0.66	1.03
32	U56822	Rattus norveg Ly-49.12 antigen mRNA, co	0.85	1.22	0.75	0.76	0.41	**0.16**	0.70	0.87
33	NM_013160	Max interacting protein 1	0.54	0.82	0.93	0.70	0.29	**0.36**	0.62	0.48
34	J03624	Galanin	0.90	0.94	0.60	0.56	0.47	**0.06**	0.58	0.56
35	NM_017042	Protein phosphatase 3, catalytic subunit, β i	0.91	1.25	0.85	0.68	0.90	**0.06**	0.73	0.46
36	NM_019270	K+ volt gated chan, shaker related subfam,	0.86	1.13	0.65	0.62	0.47	**0.31**	0.64	0.51
37	D82928	CDP-diacylglycerol-inositol 3-phosphatidylt	0.88	0.79	0.13	0.68	0.27	**0.05**	0.56	0.59
38	M27883	Rat pancreat secretory trypsin inhib II RNA,	1.48	0.43	0.23	0.46	1.21	**0.05**	0.50	0.37
39	NM_012501	Apolipoprotein C-3	1.39	0.75	0.32	0.50	1.07	**0.03**	0.45	0.22
40	NM_133552	Williams-Beuren syndr chromos region 14	1.22	1.21	1.35	1.52	1.29	0.98	**0.08**	0.88
41	NM_016999	P450, subfamily IVB, polypeptide 1	1.15	1.02	1.08	0.47	0.80	0.52	0.34	**0.15**
42	NM_019174	carbonic anhydrase 4	1.29	1.42	1.63	0.61	0.77	5.78	1.14	**0.09**
43	AF115768	Rat defensin-5 precursor mRNA, partial c	0.86	2.09	1.33	1.00	0.47	0.63	0.58	**0.44**
44	NM_013131	Mineralocorticoid receptor	0.64	0.99	0.58	0.65	0.44	0.53	0.64	**0.31**
45	AF052695	Cell cycle protein p55CDC	0.85	0.83	0.70	0.88	0.46	0.52	0.70	**0.06**
46	NM_012537	P450 (11-beta-hydroxylase)	0.83	0.77	0.06	0.90	1.11	0.62	1.22	1.40
47	AI144785	ESTs, sim to TIAM_MOUSE T-lymphoma i	1.24	3.39	4.10	2.06	2.76	3.58	2.59	0.87
48	NM_012591	Interferon regulatory factor 1	9.80	0.72	1.13	1.24	1.47	1.27	1.49	1.69
49	NM_019134	Solute carrier family 12, member 1	4.74	6.98	10.74	5.03	4.65	0.24	0.99	1.76
50	NM_144737	flavin containing monooxygenase 2	1.47	1.21	1.70	1.43	0.59	0.38	0.48	0.38
51	AB023781	Cathepsin Y	0.63	0.86	0.62	0.62	0.39	0.42	0.48	0.55

The 51 listed genes satisfied the criterion of an overall effect, and the first 45 of them also satisfied the other criterion of an effect in a 2-group test at 1 or more time points posthemorrhage (statistical analyses of microarrays analyses). Column headings at *right* include the times (h) after hemorrhage (H). Nos. are the folding values (geometric mean Cy5/Cy3 ÷ geometric mean for reference group Cy5/Cy3: upregulation, >1; downregulation, <1). Con, control; Sh, sham hemorrhage. Comparisons that were significant by both criteria are indicated by bold.

genes with the lowest obtainable FDR ($q = 0.11$). With consideration of only the two-group comparisons, 425 genes were significantly altered at one or more time points vs. sham ($q < 0.05$). There were 45 genes meeting both criteria and thus identified with a statistically detectable change after hemorrhage (Table 3). No genes were detected in this manner as changed in comparisons of Con vs. Sh, H1h vs. Sh, and H16h vs. Sh. There were no genes with a detected posthemorrhage elevated expression at one time point and a reduced expression at another. Detectable upregulation occurred in 12 genes (at 3 or more time points in 3 of them) and downregulation in 33 genes (at 3 or more time points in 12 of them). None of the cases within any RGNC met the criteria for a detectable change after hemorrhage.

Cluster analysis is another method for evaluating gene expression data, and, although not providing statistical comparisons, it organizes large amounts of data in a readily assessable format, grouping genes together according to similarities of their pattern of expression. Hierarchical clustering (8) was performed on the 425 genes passing the SAM two-group test at one or more time points vs. Sh. The cluster view in Fig. 5 shows grouping into patterns of up- or downregulation, the former involving a little less than half the 425 genes. Because acceptance of a gene for clustering required only a significant alteration at one time point, this approach allows the appreciation of similar patterns among genes in a wider pool than offered by the more-stringent double criterion we set for statistical detection of a change. With the exception of a small cluster at the start of the cluster view, suggesting a component of downregulation, most genes appeared either exclusively up or down in regulation. This is in conformity with the patterns seen among the 45 genes whose changes were more stringently detectable.

Figure 6 shows genes apparently upregulated in three patterns, indicating the possibility of genes working together. Figure 6*A* shows a cluster of genes, previously associated with leukocytes, that would represent leukocytes having immigrated into the lung and/or may indicate a tendency for increased vascularity resulting from the hypoxia of global ischemia induced by hemorrhage. Calgranulin B and neutrophil collagenase are known to be part of the transcriptome of the neutrophil. Though the increased numbers of neutrophils suggested histologically were not definitive, a rise in myeloperoxidase activity was evident. Genes for a variety of growth factors associated with monocytes, such as IL-18, placental growth factor, and fibroblast growth factor, were also in this cluster. Genes for placental growth factor, angiopoetin-1, and fibroblast growth factor 12, implicated in angiogenesis, appeared upregulated early and remained relatively high during the 72 h after hemorrhage.

Figure 6*B* indicates a requirement for increased protein synthesis, as many ribosomal proteins appear upregulated in expression. In addition, the increased expression of thioredoxin and xanthine oxidase suggests redox alterations in some cells. Most of the alterations in gene expression in this cluster have returned to normal by 72 h.

Figure 6*C* shows a cluster of genes whose elevation in expression occurs early and remains high for the entire 72 h. The early and sustained elevation of pyruvate dehydrogenase kinase, a nuclear coded mitochondrial protein that inactivates the pyruvate dehydrogenase complex, indicates a reduction in production of ATP via acetyl-CoA metabolism and would tend to reduce generation of oxidation products resulting from incomplete oxidation under conditions of hypoxia.

Figure 7 indicates RT-PCR confirmation of upregulatory gene responses to hemorrhage in a subset of eight genes with upregulation on microarrays as depicted in the cluster results (Fig. 6). Together, these genes allow appreciation of a correlation between the methods.

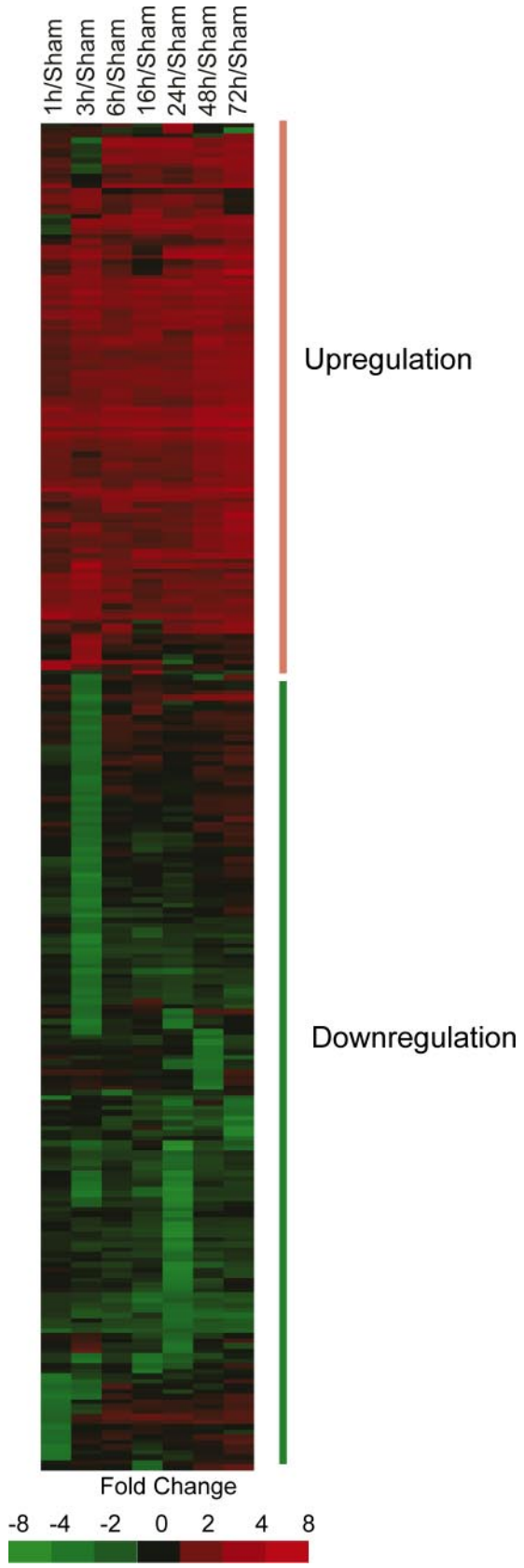

Fig. 5. Cluster image showing alterations in gene expression of the 425 genes passing the statistical analysis of microarrays (SAM) 2-group test relative to sham at some time during the period of recovery from hemorrhage.

DISCUSSION

Prevention of the development of acute lung injury following hemorrhage requires a molecular understanding of the response of the lung. The aim of this study was to understand

Fig. 6. Temporal patterns of the upregulated genes (from Fig. 5) in rat lung after hemorrhage. *A*: gene clusters associated with immune cell trafficking in the lung after hemorrhage. The presence of interleukin 18 and interleukin 2 indicates that monocytes and T cells may also be present in lung following hemorrhage. *B*: gene clusters implicated in redox alterations and protein synthesis. *C*: gene clusters associated with metabolic regulation.

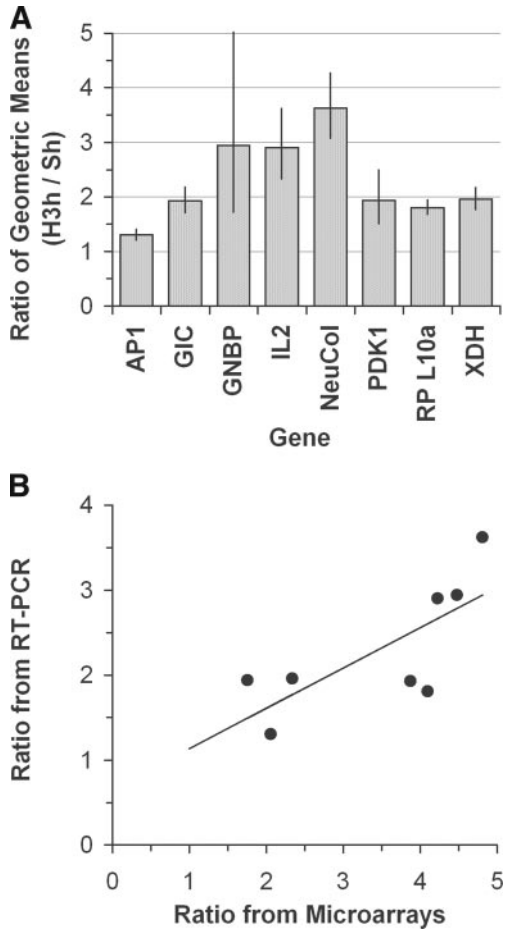

Fig. 7. *A*: fold change by RT-PCR 3 h posthemorrhage for 8 genes representing the 3 gene clusters shown in Fig 6. The error lines represent the standard error of the difference (H3h minus Sh) between the separate-group means of the logs of the normalized values for intensities, displayed on the unlogged ordinate scale to represent variation of the ratios of geometric means. Neutral response would be the ordinate value 1, and all responses were statistically significant ($P < 0.05$ or $P < 0.01$) except those for GNBP and PDK1. AP1, angiopoietin 1; GIC, L-gicerin; GNBP, guanine nucleotide binding protein gamma 7; IL2, interleukin 2; NeuCol, neutrophil collagenase; PDK1, pyruvate dehydrogenase kinase 1; RP L10a, ribosomal protein L10a; XDH, xanthine dehydrogenase; Sh, sham hemorrhage; h, hours; H, hemorrhage. *B*: ratio (H3h/Sh) of geometric means (folding change) correlated ($r = 0.744$, $P = 0.034$) between RT-PCR and microarray results for the 8 genes depicted in *A*. Each gene passed the SAM 2-group test for upregulation on microarrays at either 3 h or 6 h posthemorrhage or both.

the response of lung to global ischemia as present in severe hemorrhage, uncomplicated by other trauma, anesthesia, or resuscitation. Although the hemorrhage was severe, all animals survived. McGlew et al. (16), working with a conscious model in which variable amounts of blood were removed over a 20-min period, demonstrated that 2.5 ml/100 g resulted in 74% survival at 24 h and 2.75 ml/100 g resulted in 46% survival at 24 h. Withdrawal of 3.0 ml over a 20-min period resulted in only 20% survival at 24 h. Although blood (2.6 ml/100 g) was removed more rapidly in the present study, no rats died, possibly because they were fully recovered from the instrumentation surgery. Heparin was removed 24 h before hemorrhage and should not be a confounding factor in these studies, since previous studies have shown that heparin improves survival after hemorrhage (38, 39).

In evaluating genomic data, we thought that a severe, but not lethal, hemorrhage might be important, because gene expression profiling with microarrays requires good-quality RNA. In preliminary model development experiments, RNA from animals close to death exhibited considerable degradation, and degraded RNA may confound results. In addition, resuscitation seems to add another variable to the response to hemorrhage. It has been shown that resuscitation with lactated Ringer's solution or hetastarch can activate neutrophils (Rhee et al., Ref. 21), cause apoptosis in small intestine and liver (6), elevate ICAM-1 and VCAM-1, and also stimulate expression of E- and P-selectins (5, 29), thereby initiating a proinflammatory state. Therefore, no resuscitation was used in the present study.

Nonspecific hybridization was assessed in two ways: by use of buffer spots (blanks) and spots of oligonucleotides with nonspecific sequences (RGNCs) provided by the manufacturer of the oligonucleotides. The two estimates from different techniques, both suggesting detectable activity in the range of ~90% of rat lung genes, are similar, providing confidence that the changes seen in our analysis represented real differences.

The overall within- and between-array CV estimates for Cy5, Cy3, and Cy5/Cy3 were between 20 and 33%. Assay variability and the typically low sample replication so far remain wide-spread exigencies for microarray profiling. These factors probably contribute to limitation of the number of genes that a statistical program can detect as altered in regard to a given FDR. It should be noted that, since there was one microarray per rat, the between-array CV estimates for Cy5 (33%), Cy3 (20%), and their ratio (26%) include between-rat variation.

We considered the genes passing both the multigroup test and at least one two-group test to constitute the final list of genes with a statistically detected posthemorrhage alteration (Table 3). The most highly upregulated gene on this list was for neutrophil collagenase, suggesting highly active white cells in the lung after hemorrhage. The changes seen in the numbers of neutrophils in the blood corroborate this finding. There is an early (by 1 h) reduction of the number of the neutrophils in blood, which could be due to extravasation into the tissues, including lung. Ensuing increases in gene expression became significant at 3 h. There was a large increase in the total number of circulating neutrophils at 72 h, and the high neutrophil-related gene expression, maximum at 72 h, indicates the collection of neutrophils in the lung or its vasculature. Genes for a calcium-binding protein and a Ca-ATPase were also among the 12 detected as upregulated, suggesting increased cellular activity related to intracellular calcium signaling. No genes appeared to be up- and downregulated at different times. Downregulation was detected in 33 genes, including those for a G protein-coupled receptor, arginine vasopressin receptor 1B, two potassium channels, and the mineralocorticoid receptor, suggesting changes related to endocrine function compensating for hemorrhage. Vasoconstriction almost certainly helped lead to the correction of MAP (13), and there were shifts in fluid compartment composition (17) consistent with the known compensatory responses to hemorrhage. The increase in protein in the plasma may reflect a generalized increase in synthesis by a number of tissues and suggests that the increase in gene expression of ribosomal proteins might result in increased protein synthetic activity.

The purpose of microarray analysis is to screen a large number of genes for a change, to produce a short list of genes maximizing the efficiency of subsequent testing. Even with the threshold effect size set to produce a given estimated FDR (here, 5% for any one two-group test), the analyses are unable to determine which of the detected changes are false. We provide a list of 45 genes (shortened from the total 5,671) that might be explored in further studies with an expected high yield of changes due to hemorrhage. The overall reliability of such statistically based expectations is not yet known, but quantification of that reliability will depend on an adequate extent of follow-on studies with conventional tests focused more narrowly on specific genes with greater sampling replication. The issue of how many truly changed genes have been left out of a short list produced by microarray analysis theoretically would be assessable, but the extent of subsequent testing with highly sensitive (but also specific) tests required to identify the false negatives would be daunting. In the meantime, it is reasonable to perform cluster analysis on a list expanded to include 425 genes passing at least the two-group test at one or more time points. Such analysis can provide information about groups of genes varying with a common time pattern (Figs. 5 and 6).

RT-PCR of a subset of genes suggested as upregulated on microarray analysis indicated significant correlation with the microarray results. This is consistent with reliability of the microarray results.

A limitation of investigating a bulk organ (lung) is the loss of information about the participation of individual cell types. While footprints of immigrating leukocytes can be discerned, the exact source of the alterations in gene expression contributed by individual cell types in the lung will require the application of techniques to isolate RNA from individual cells and their amplification before gene expression analysis. Techniques for performing such studies are emerging but have not yet become routine.

It remains to be determined the extent to which changes in gene expression result in actual changes in the protein products of the genes, a determination that would require parallel application of proteomic techniques. However, identification of genes that are likely to be changed in the context of circulatory shock, as exemplified herein, might suggest roles for genes and proteins that are heretofore unsuspected, in turn suggesting avenues for further investigation.

While the entire genomic sequences of multiple organisms are now known, it is also abundantly clear that we really know little about the function of most of these genes in any organism. One way of understanding a gene's function is to examine gene transcription in both a perturbed and normal situation and see how it changes. In the present study, the ability of oligonucleotide microarrays to detect alterations in gene expression in lung and trafficking of relatively small numbers of leukocytes was demonstrated. After severe hemorrhage, among the 425 genes appearing changed with use of a two-group test criterion alone, 45 satisfied the more-stringent combination of two criteria. Similar analysis of other tissues should identify a set of genes generally expressed following hemorrhage. Blast searches of the human genome indicate that many of the genes identified as altered in the lung in hemorrhaged rats have homologs in the human genome. Confirmation that these genes are also altered in human tissues following traumatic injury would suggest potential targets for therapeutic regulation.

DISCLOSURES

The opinions or assertions contained herein are the private views of the authors and are not to be construed as official or as reflecting the views of the Department of the Army or the Department of Defense.

REFERENCES

1. **Abraham E.** Coagulation abnormalities in acute lung injury and sepsis. *Am J Respir Cell Mol Biol* 22: 401–404, 2000.
2. **Abraham E, Bursten S, Shenkar R, Allbee J, Tuder R, Woodson P, Guidot DM, Rice G, Singer JW, and Repine JE.** Phosphatidic acid signaling mediates lung cytokine expression and lung inflammatory injury after hemorrhage in mice. *J Exp Med* 181: 569–575, 1995.
3. **Akgur FM, Zibari GB, McDonald JC, Granger DN, and Brown MF.** Effects of dextran and pentoxifylline on hemorrhagic shock-induced P-selectin expression. *J Surg Res* 87: 232–238, 1999.
4. **Alam HB, Stegalkina S, Rhee P, and Koustova E.** cDNA array analysis of gene expression following hemorrhagic shock and resuscitation in rats. *Resuscitation* 54: 195–206, 2002.
5. **Angle N, Hoyt DB, Cabello-Passini R, Herdon-Remelius C, Loomis W, and Junger WG.** Hypertonic saline resuscitation reduces neutrophil margination by suppressing neutrophil L selectin expression. *J Trauma* 45: 7–12; discussion 12–13, 1998.
6. **Ayala A, Xin Xu Y, Ayala CA, Sonefeld DE, Karr SM, Evans TA, and Chaudry IH.** Increased mucosal B-lymphocyte apoptosis during polymicrobial sepsis is a Fas ligand but not an endotoxin-mediated process. *Blood* 91: 1362–1372, 1998.
7. **Deitch EA, Xu D, Franko L, Ayala A, and Chaudry IH.** Evidence favoring the role of the gut as a cytokine-generating organ in rats subjected to hemorrhagic shock. *Shock* 1: 141–145, 1994.
8. **Faist E, Baue AE, Dittmer H, and Heberer G.** Multiple organ failure in polytrauma patients. *J Trauma* 23: 775–787, 1983.
9. **Fan J, Marshall JC, Jimenez M, Shek PN, Zagorski J, and Rotstein OD.** Hemorrhagic shock primes for increased expression of cytokine-induced neutrophil chemoattractant in the lung: role in pulmonary inflammation following lipopolysaccharide. *J Immunol* 161: 440–447, 1998.
10. **Hierholzer C, Kalff JC, Omert L, Tsukada K, Loeffert JE, Watkins SC, Billiar TR, and Tweardy DJ.** Interleukin-6 production in hemorrhagic shock is accompanied by neutrophil recruitment and lung injury. *Am J Physiol Lung Cell Mol Physiol* 275: L611–L621, 1998.
11. **Imamura M, Mikami Y, Takahashi H, and Yamauchi H.** Effect of a specific synthetic inhibitor of neutrophil elastase (ONO-5046) on the course of acute hemorrhagic pancreatitis in dogs. *J Hepatobiliary Pancreat Surg* 5: 422–428, 1998.
12. **Jarrar D, Chaudry IH, and Wang P.** Organ dysfunction following hemorrhage and sepsis: mechanisms and therapeutic approaches. *Int J Mol Med* 4: 575–583, 1999.
13. **Jochem J.** Involvement of arginine vasopressin in endogenous central histamine-induced reversal of critical haemorrhagic hypotension in rats. *Inflamm Res* 53: 269–276, 2004.
14. **Magnotti LJ, Upperman JS, Xu DZ, Lu Q, and Deitch EA.** Gut-derived mesenteric lymph but not portal blood increases endothelial cell permeability and promotes lung injury after hemorrhagic shock. *Ann Surg* 228: 518–527, 1998.
15. **Mainous MR, Ertel W, Chaudry IH, and Deitch EA.** The gut: a cytokine-generating organ in systemic inflammation? *Shock* 4: 193–199, 1995.
16. **McGlew MJ, Safar P, and Stremple P.** A simple survival model of volume-controlled hemorrhagic shock in awake rats. *Resuscitation* 21: 247–257, 1991.
17. **Moon PF, Hollyfield-Gilbert MA, Myers TL, Uchida T, and Kramer GC.** Fluid compartments in hemorrhaged rats after hyperosmotic crystalloid and hyperoncotic colloid resuscitation. *Am J Physiol Renal Fluid Electrolyte Physiol* 270: F1–F8, 1996.
18. **Mulligan MS, Desrochers PE, Chinnaiyan AM, Gibbs DF, Varani J, Johnson KJ, and Weiss SJ.** In vivo suppression of immune complex-induced alveolitis by secretory leukoproteinase inhibitor and tissue inhibitor of metalloproteinases 2. *Proc Natl Acad Sci USA* 90: 11523–11527, 1993.

19. **Parsey MV, Kaneko D, Shenkar R, and Abraham E.** Neutrophil apoptosis in the lung after hemorrhage or endotoxemia: apoptosis and migration are independent of IL-1β. *Clin Immunol* 91: 219–225, 1999.
20. **Pope A, French G, and Longneckar DE.** *Fluid Resuscitation: State of the Science for Treating Combat Casualties and Civilian Injuries (1999)*. Washington, DC: National Academy, 1999.
21. **Rhee P, Burris D, Kaufmann C, Pikoulis M, Austin B, Ling G, Harviel D, and Waxman K.** Lactated Ringer's solution resuscitation causes neutrophil activation after hemorrhagic shock. *J Trauma* 44: 313–319, 1998.
22. **Sambol JT, Xu DZ, Adams CA, Magnotti LJ, and Deitch EA.** Mesenteric lymph duct ligation provides long term protection against hemorrhagic shock-induced lung injury. *Shock* 14: 416–419; discussion 419–420, 2000.
23. **Sauaia A, Moore FA, Moore EE, Moser KS, Brennan R, Read RA, and Pons PT.** Epidemiology of trauma deaths: a reassessment. *J Trauma* 38: 185–193, 1995.
24. **Schmid E, Piccolo MT, Friedl HP, Warner RL, Mulligan MS, Hugli TE, Till GO, and Ward PA.** Requirement for C5a in lung vascular injury following thermal trauma to rat skin. *Shock* 8: 119–124, 1997.
25. **Shackford SR, Mackersie RC, Holbrook TL, Davis JW, Hollingsworth-Fridlund P, Hoyt DB, and Wolf PL.** The epidemiology of traumatic death. A population-based analysis. *Arch Surg* 128: 571–575, 1993.
26. **Shenkar R and Abraham E.** Hemorrhage induces rapid in vivo activation of CREB and NF-κB in murine intraparenchymal lung mononuclear cells. *Am J Respir Cell Mol Biol* 16: 145–152, 1997.
27. **Shenkar R and Abraham E.** Mechanisms of lung neutrophil activation after hemorrhage or endotoxemia: roles of reactive oxygen intermediates, NF-κB, and cyclic AMP response element binding protein. *J Immunol* 163: 954–962, 1999.
28. **Shenkar R and Abraham E.** Plasma from hemorrhaged mice activates CREB and increases cytokine expression in lung mononuclear cells through a xanthine oxidase-dependent mechanism. *Am J Respir Cell Mol Biol* 14: 198–206, 1996.
29. **Shenkar R, Cohen AJ, Vestweber D, Miller YE, Tuder R, and Abraham E.** Hemorrhage and resuscitation alter the expression of ICAM-1 and P-selectin in mice. *J Inflamm* 45: 248–259, 1995.
30. **Shenkar R, Coulson WF, and Abraham E.** Hemorrhage and resuscitation induce alterations in cytokine expression and the development of acute lung injury. *Am J Respir Cell Mol Biol* 10: 290–297, 1994.
31. **Smail N, Catania RA, Wang P, Cioffi WG, Bland KI, and Chaudry IH.** Gut and liver: the organs responsible for increased nitric oxide production after trauma-hemorrhage and resuscitation. *Arch Surg* 133: 399–405, 1998.
32. **Storey JD and Tibshirani R.** Statistical significance for genomewide studies. *Proc Natl Acad Sci USA* 100: 9440–9445, 2003.
33. **Trush MA, Egner PA, and Kensler TW.** Myeloperoxidase as a biomarker of skin irritation and inflammation. *Food Chem Toxicol* 32: 143–147, 1994.
34. **Tusher VG, Tibshirani R, and Chu G.** Significance analysis of microarrays applied to the ionizing radiation response. *Proc Natl Acad Sci USA* 98: 5116–5121, 2001.
35. **Upperman JS, Deitch EA, Guo W, Lu Q, and Xu D.** Post-hemorrhagic shock mesenteric lymph is cytotoxic to endothelial cells and activates neutrophils. *Shock* 10: 407–414, 1998.
36. **Ventura SJ, Peters KD, Martin JA, and Maurer JD.** Births and deaths: United States, 1996. *Mon Vital Stat Rep* 46: 1–40, 1997.
37. **Wang P, Ba ZF, Biondo A, and Chaudry IH.** Liver endothelial cell dysfunction occurs early following hemorrhagic shock and persists despite crystalloid resuscitation. *J Surg Res* 63: 241–247, 1996.
38. **Wang P, Ba ZF, and Chaudry IH.** Endothelial cell dysfunction occurs after hemorrhage in nonheparinized but not in preheparinized models. *J Surg Res* 54: 499–506, 1993.
39. **Watkins JM, Spain DA, Krysztopik RJ, Downard PJ, Wilson MA, and Garrison RN.** Heparan preserves intestinal perfusion after hemorrhage and resuscitation. *J Surg Res* 66: 154–158, 1996.
40. **Xiang CC, Kozhich OA, Chen M, Inman JM, Phan QN, Chen Y, and Brownstein MJ.** Amine-modified random primers to label probes for DNA microarrays. *Nat Biotechnol* 20: 738–742, 2002.
41. **Younger JG, Taqi AS, Jost PF, Till GO, Johnson KJ, Stern SA, and Hirschl RB.** The pattern of early lung parenchymal and air space injury following acute blood loss. *Acad Emerg Med* 5: 659–665, 1998.
42. **Zallen G, Moore EE, Johnson JL, Tamura DY, Ciesla DJ, and Silliman CC.** Posthemorrhagic shock mesenteric lymph primes circulating neutrophils and provokes lung injury. *J Surg Res* 83: 83–88, 1999.